

EUR 3335. e

EUROPEAN ATOMIC ENERGY COMMUNITY — EURATOM

**INFLUENCE OF NEUTRON IRRADIATION
ON THE MECHANICAL PROPERTIES
AND THE CORROSION BEHAVIOUR
OF $ZrNb_3Sn$ AND ZIRCALOY-2**

by

H. RICHTER and W. RUCKDESCHEL
(Metallgesellschaft AG, Frankfurt/Main)

and

W. SPALTHOFF and E. STARKE
(G. K. S. S. mbH, Geesthacht)

1967



EURATOM/US Agreement for Cooperation

**EURAEK Report No. 1795 prepared by
Metallgesellschaft AG, Metall-Laboratorium, Frankfurt/Main, Germany**

Euratom Contract No. 092-62-7 RDD

Paper presented at the
International Conference on the Use of Zirconium Alloys in Nuclear Reactors
Pilsen, Czecho-Slovakia, October 20-21, 1966

LEGAL NOTICE

This document was prepared under the sponsorship of the Commission of the European Atomic Energy Community (Euratom) in pursuance of the joint programme laid down by the Agreement for Cooperation signed on 8 November 1958 between the Government of the United States of America and the European Atomic Energy Community.

It is specified that neither the Euratom Commission, nor the Government of the United States, their contractors or any person acting on their behalf :

Make any warranty or representation, express or implied, with respect to the accuracy; completeness, or usefulness of the information contained in this document, or that the use of any information, apparatus, method, or process disclosed in this document may not infringe privately owned rights; or

Assume any liability with respect to the use of, or for damages resulting from the use of any information, apparatus, method or process disclosed in this document.

This report is on sale at the addresses listed on cover page 4

at the price of FF 5.—	FB 50	DM 4.—	Lit. 620	Fl. 3.60
------------------------	-------	--------	----------	----------

When ordering, please quote the EUR number and the title, which are indicated on the cover of each report.

Printed by VAILLANT-CARMANNE
Brussels, May 1967

EUR 3335.e

INFLUENCE OF NEUTRON IRRADIATION ON THE MECHANICAL PROPERTIES AND THE CORROSION BEHAVIOUR OF ZrNb₃Sn₁ AND ZIRCALOY-2 by H. RICHTER and W. RUCKDESCHEL Metallgesellschaft AG, Frankfurt/Main) and W. SPALTHOFF and E. STARKE (G. K. S. S. mbH, Geesthacht)

European Atomic Energy Community — EURATOM

Euratom/US Agreement for Cooperation

EURAEK Report No. 1795 prepared by Metallgesellschaft AG,

Metall-Laboratorium Frankfurt/Main, Germany

Euratom Contract No. 092-62-7 RDD

Paper presented at the International Conference on the Use of Zirconium Alloys in Nuclear Reactors — Pilsen, Czecho-Slovakia, October 20-21, 1966
Brussels, May 1967 — 32 Pages — 19 Figures — FB 50

The effect of neutron irradiation on mechanical and corrosion properties of the alloys ZrNb₃Sn₁ and zircaloy-2 was tested at the swimmingpool reactor FRG-1. Tensile and impact specimens were subjected to an integrated fast

EUR 3335.e

INFLUENCE OF NEUTRON IRRADIATION ON THE MECHANICAL PROPERTIES AND THE CORROSION BEHAVIOUR OF ZrNb₃Sn₁ AND ZIRCALOY-2 by H. RICHTER and W. RUCKDESCHEL Metallgesellschaft AG, Frankfurt/Main) and W. SPALTHOFF and E. STARKE (G. K. S. S. mbH, Geesthacht)

European Atomic Energy Community — EURATOM

Euratom/US Agreement for Cooperation

EURAEK Report No. 1795 prepared by Metallgesellschaft AG,

Metall-Laboratorium Frankfurt/Main, Germany

Euratom Contract No. 092-62-7 RDD

Paper presented at the International Conference on the Use of Zirconium Alloys in Nuclear Reactors — Pilsen, Czecho-Slovakia, October 20-21, 1966
Brussels, May 1967 — 32 Pages — 19 Figures — FB 50

The effect of neutron irradiation on mechanical and corrosion properties of the alloys ZrNb₃Sn₁ and zircaloy-2 was tested at the swimmingpool reactor FRG-1. Tensile and impact specimens were subjected to an integrated fast

flux ($E > 1$ MeV) of up to $4.5 \cdot 10^{19}$ n/cm² at 45° C in contact with the pool water. Corrosion specimens were irradiated in autoclaves in steam of 400 °C and 100 at for up to 820 hours; in this case the maximum integrated fast flux ($E > 1$ MeV) was $1.5 \cdot 10^{19}$ n/cm². For comparison, analogous tests without irradiation have been performed. The radiation caused an additional enhancement of the hydrogen uptake. The enhancement factors for the weight gains are not very well established, but there are indications that ZrNb3Sn1 is more corrosion-resistant under irradiation than zircaloy-2. With both alloys the irradiation increases the yield strength and the ultimate tensile strength and decreases the elongation. The impact strength of ZrNb3Sn1 was increased but that of zircaloy-2 was not essentially altered by the irradiation. The mechanical properties of both alloys reach saturation values with an integrated fast flux of about $3 \cdot 10^{19}$ n/cm².

The recovery of radiation damage was investigated up to 450° C. While a 2 h-anneal at 300° C had no effect on the mechanical properties, a short anneal at 450° C was sufficient to eliminate the total irradiation-hardening.

flux ($E > 1$ MeV) of up to $4.5 \cdot 10^{19}$ n/cm² at 45° C in contact with the pool water. Corrosion specimens were irradiated in autoclaves in steam of 400 °C and 100 at for up to 820 hours; in this case the maximum integrated fast flux ($E > 1$ MeV) was $1.5 \cdot 10^{19}$ n/cm². For comparison, analogous tests without irradiation have been performed. The radiation caused an additional enhancement of the hydrogen uptake. The enhancement factors for the weight gains are not very well established, but there are indications that ZrNb3Sn1 is more corrosion-resistant under irradiation than zircaloy-2. With both alloys the irradiation increases the yield strength and the ultimate tensile strength and decreases the elongation. The impact strength of ZrNb3Sn1 was increased, but that of zircaloy-2 was not essentially altered by the irradiation. The mechanical properties of both alloys reach saturation values with an integrated fast flux of about $3 \cdot 10^{19}$ n/cm².

The recovery of radiation damage was investigated up to 450° C. While a 2 h-anneal at 300° C had no effect on the mechanical properties, a short anneal at 450° C was sufficient to eliminate the total irradiation-hardening.

EUR 3335. e

EUROPEAN ATOMIC ENERGY COMMUNITY — EURATOM

**INFLUENCE OF NEUTRON IRRADIATION
ON THE MECHANICAL PROPERTIES
AND THE CORROSION BEHAVIOUR
OF ZrNb₃Sn₁ AND ZIRCALOY-2**

by

H. RICHTER and W. RUCKDESCHEL
(Metallgesellschaft AG, Frankfurt/Main)

and

W. SPALTHOFF and E. STARKE
(G. K. S. S. mbH, Geesthacht)

1967



EURATOM/US Agreement for Cooperation

**EURAEK Report No. 1795 prepared by
Metallgesellschaft AG, Metall-Laboratorium, Frankfurt/Main, Germany**

Euratom Contract No. 092-62-7 RDD

Paper presented at the
International Conference on the Use of Zirconium Alloys in Nuclear Reactors
Pilsen, Czecho-Slovakia, October 20-21, 1966

SUMMARY

The effect of neutron irradiation on mechanical and corrosion properties of the alloys ZrNb3Sn1 and zircaloy-2 was tested at the swimmingpool reactor FRG-1. Tensile and impact specimens were subjected to an integrated fast flux ($E > 1$ MeV) of up to $4.5 \cdot 10^{19}$ n/cm^2 at 45° C in contact with the pool water. Corrosion specimens were irradiated in autoclaves in steam of 400° C and 100 at for up to 820 hours; in this case the maximum integrated fast flux ($E > 1$ MeV) was $1.5 \cdot 10^{19}$ n/cm^2 . For comparison, analogous tests without irradiation have been performed. The radiation caused an additional enhancement of the hydrogen uptake. The enhancement factors for the weight gains are not very well established, but there are indications that ZrNb3Sn1 is more corrosion-resistant under irradiation than zircaloy-2. With both alloys the irradiation increases the yield strength and the ultimate tensile strength and decreases the elongation. The impact strength of ZrNb3Sn1 was increased, but that of zircaloy-2 was not essentially altered by the irradiation. The mechanical properties of both alloys reach saturation values with an integrated fast flux of about $3 \cdot 10^{19}$ n/cm^2 .

The recovery of radiation damage was investigated up to 450° C. While a 2 h-anneal at 300° C had no effect on the mechanical properties, a short anneal at 450° C was sufficient to eliminate the total irradiation-hardening.

CONTENTS

1 — INTRODUCTION	5
2 — PROPERTIES OF ZrNb ₃ Sn ₁	6
3 — EXPERIMENTAL	8
3.1 — Material and Fabrication of Specimens	8
3.2 — Irradiation Experiments	14
3.3 — Examination of Irradiated Specimens	16
3.4 — Comparative Tests without Irradiation	16
4 — CORROSION BEHAVIOUR UNDER IRRADIATION	17
4.1 — Results	17
4.2 — Discussion	23
5 — MECHANICAL PROPERTIES AFTER IRRADIATION	25
5.1 — Results	25
5.2 — Discussion	27
6 — INVESTIGATION OF RECOVERY	28
6.1 — Results	28
6.2 — Discussion	29
REFERENCES	29

KEY TO THE TABLES

- I. Analysis of base materials used for vacuum melting ZrNb₃Sn₁.
- II. Chemical composition of the billets.
- III. Fabrication and heat-treatment of both alloys.
- IV. Spectral distribution of neutron fluxes.
- V. Weight gains and hydrogen uptake in 400° C steam with and without radiation.
- VI. Enhancement of oxidation in sealed autoclaves with and without radiation.

KEY TO THE FIGURES

1. Creep behaviour of the alloys ZrNb3Sn1, ZrNb2, and zircaloy-2.
2. Corrosion of ZrNb3Sn1, ZrNb2 and zircaloy-2 in water (350° C) and steam (400° C, 480° C).
3. Influence of heat-treatment on the weight gains during steam corrosion.
4. Dimensions of specimens for the irradiation tests.
5. Microsections of zircaloy-2 specimens.
6. Microsections of ZrNb3Sn1 specimens.
7. Impact energy curves for various specimen orientations of zirconium.
8. Positions of the specimen containers in the reactor FRG-1.
9. Capsules for irradiation experiments.
10. Weight gains of zircaloy-2 and ZrNb3Sn1 during steam-corrosion at 400° C (without irradiation, frequent water exchange).
11. Tensile specimens after in-pile corrosion.
12. Hydrides in zircaloy-2 sheet after steam-corrosion (400° C) with and without irradiation.
13. Hydrides in ZrNb3Sn1 sheet after steam-corrosion (400° C) with and without irradiation.
14. Mechanical properties of zircaloy-2 and ZrNb3Sn1 after steam-corrosion with and without irradiation.
15. Influence of irradiation on the mechanical properties of zircaloy-2 and ZrNb3Sn1.
16. Effect of integrated fast flux on the mechanical properties.
17. Effect of irradiation and additional heat-treatment on impact strength.
18. Ultimate tensile strength of welded sheet specimens after irradiation.
19. The recovery of irradiation damage as a function of temperature.

INFLUENCE OF NEUTRON IRRADIATION ON THE CORROSION BEHAVIOUR AND THE MECHANICAL PROPERTIES OF ZrNb3Sn1 AND ZIRCALOY-2 (*)

I — Introduction

These investigations are part of a development program sponsored by EURATOM (1) and started in 1960. At that time, the knowledge of zircaloy-2 (an alloy with 1.5 % Sn and 0.3 % Fe + Cr + Ni) had already significantly advanced. This alloy, being also competitive with stainless steel on account of its low capture cross section for thermal neutrons, had a good chance to be applied in water- and steam-cooled reactors (2). At coolant temperatures of up to 300° C, the corrosion resistance and mechanical properties of this alloy render it very suitable for the use in thin-walled canning tubes and structural parts of the cores.

In 1958, at the Geneva Conference, some Russian investigations were reported, dealing with binary and complex zirconium alloys for water and steam application (3-5). The alloying elements used for these investigations had been Al, Cr, Fe, Mo, Nb, Ni, Sn, Ta, Ti, V and W. Niobium additions proved to increase the strength and creep resistance remarkably. At the same time, the corrosion resistance of iodide zirconium in pressurized water of up to 350° C was improved by niobium additions. For application at elevated temperatures (water 350° C, steam 400° C), alloys of the «Ozhennite»-type containing 0.1 - 0.2 % Sn and 0.1 % each of Fe, Nb and Ni seemed to be very promising.

Also in western countries, especially in the USA, the strengthening effect of niobium additions had been investigated (6-13). Among the 29 alloys tested by Schwöpe and Chubb (9) a binary alloy with 2.2 % Nb was one of the best regarding the yield strength at 500° C. The corrosion resistance was at least not deteriorated by niobium additions (in 315° C-steam : 11).

Starting from these promising aspects, the Metallgesellschaft AG proposed to EURATOM a development program for advanced zirconium alloys in 1959. The properties of these alloys should be sufficient for reactor application in pressurized water of up to 350° C and in steam of up to 400° C. The corrosion resistance at elevated temperatures had to be better than that of zircaloy-2. At conventional temperatures, the strength should be superior to that of zircaloy-2, and the corrosion resistance equal or better. The scope of alloys included binary ZrNb alloys and ternary ZrNb alloys with additions of Cr, Pd, Mo, Si and, especially, Sn. The results of the first test series compelled us to renounce compositions with Cr, Pd, and Mo and narrowed the field of promising alloys to ternary ZrNbSn alloys (14). The final selection of the alloy ZrNb3Sn1 with 3 weight-% Nb and 1 weight-% Sn was based on the high strength and creep resistance and on the agreeable corrosion resistance after an appropriate final heat-treatment (see chap. 2). The arguments for this selection are discussed by K. Anderko *et al.* (15).

(*) Manuscript received on October 17, 1966.

The continued research on the ZrNb3Sn1 alloy included detailed corrosion studies, investigations of the influence of hydrogen on the structure and the mechanical properties (16, 17), studies of the ternary phase diagram (17, 18), and technological development work (welding, workability and properties of canning-tubes (17,19)). The workability of this alloy proved to be similar to that of zircaloy-2. Thin-walled, seamless tubes, sheets and foils can be produced regardless of the increased strength. The usual welding processes as TIG with trailer shield or in chambers and electron-beam welding can be applied for joints.

Besides these data, detailed information of the effect of neutron-irradiation on the mechanical properties and the corrosion behaviour of this alloy was desired before taking the last step, i.e. nuclear application. These investigations were sponsored by EURATOM under contract No. 092-62-7 RDD and were accomplished by the Metall-Laborium of Metallgesellschaft AG, Frankfurt (Main), in cooperation with Gesellschaft für Kernenergieverwertung in Schiffbau und Schifffahrt mbH, Hamburg, operating the reactor FRG-1 which was used for the in-pile tests (reported : 22, 56).

2 — Properties of ZrNb3Sn1

Before discussing the in-pile behaviour, a short review of the mechanical properties and the corrosion behaviour will be useful.

The strength of ZrNb3Sn1 is higher than that of ZrNb2.5 caused by the additional 0.5 % Nb and by the tin content. For technical applications, especially under higher mechanical stresses, for example in pressure tubes, the creep behaviour is a very important factor. In Fig. 1 the creep-strengths of zircaloy-2, ZrNb2, and ZrNb3Sn1 are compared. In the conventional temperature -range of up to 350° C, ZrNb3Sn1 has the highest creep strength. Above 400° C, this advantage is less conspicuous.

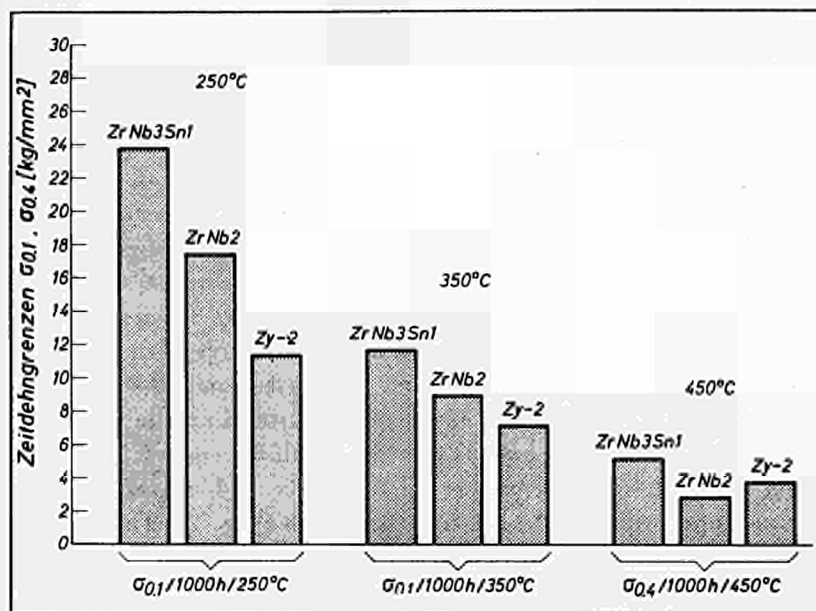


FIG. 1 — Creep behaviour of the alloys ZrNb3Sn1, ZrNb2 and zircaloy-2 (0.1 % and 0.4 % creep def. limit $\sigma_{0.1/1000 \text{ hr}}$ and $\sigma_{0.4/1000 \text{ hr}}$).

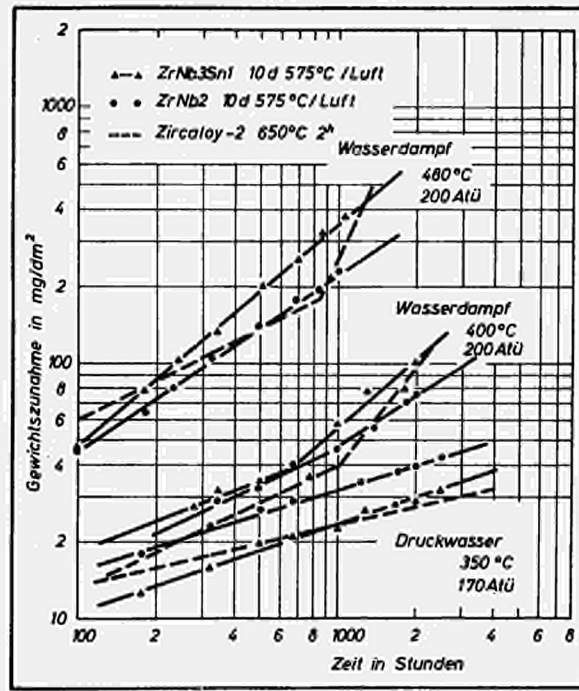


FIG. 2 — Corrosion of ZrNb3Sn1, ZrNb2 and zircaloy-2 in water (350° C) and steam (400° C, 480° C).

Fig. 2 shows the weight gains of zircaloy-2 and ZrNb-alloys during corrosion in pressurized water and steam. At 350° C, the corrosion rate of ZrNb3Sn1 is as low as that of zircaloy-2 and lower than that of ZrNb2. Contrary thereto, Ivanov and Grigorovich (4) reported that Nb contents above 1 wt.-% were detrimental to corrosion. Douglass (55) also stated weight gains of ZrNb and ZrNbSn alloys which were by several times higher than those of zircaloy-2. These contradictions may be explained by the different heat-treatments.

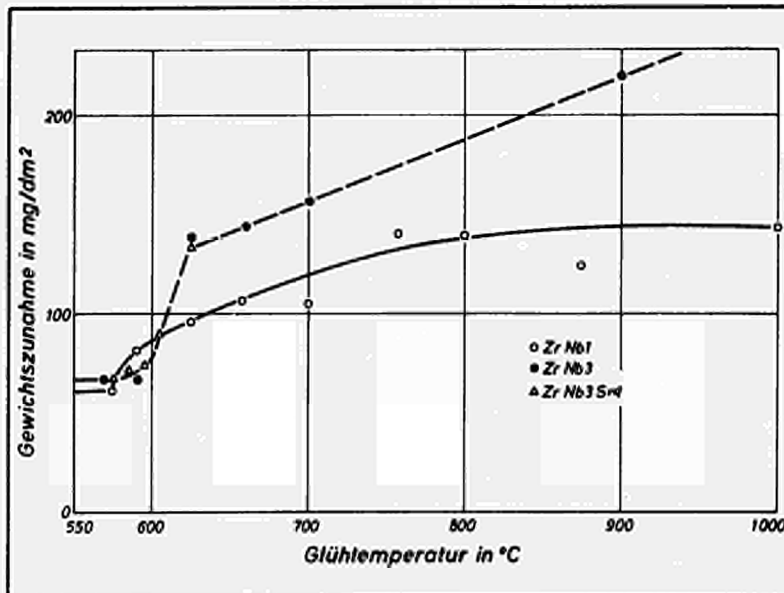


FIG. 3 — Influence of heat-treatment on the weight gains during steam corrosion (1720 hr at 400° C).

The corrosion of ZrNb-alloys is very sensitive to the final heat-treatment (Fig. 3). The anneal must be performed below the monotectoid temperature for a sufficient length of time to precipitate such an amount of the β_{Nb} phase as is necessary to obtain thermodynamic equilibrium. After the most favourable anneal of 16 hours at 540° C, the weight gains of canning tubes at 400° C have been similar to those of zircaloy-2 (24).

3 — Experimental

3.1 — Material and Fabrication of Specimens

The electrodes for the vacuum melting-process consisted of zirconium sponge of reactor grade quality (analysis Table Ia) and key alloys containing niobium with a low content of interstitials (analysis Table Ib) and tin (99.99 %), or tin, chromium, iron and nickel. The analysis of the double arc-melted ingots (85 mm diameter) proves the homogeneity of the material (Table II). The fabrication schedule is listed in Table III.

TABLE I

Analysis of base materials used for vacuum melting ZrNb3Sn1

a) zirconium sponge, impurities :

Element	Content in ppm	Element	Content in ppm
Al	70	Mg	50
B	0.5	Mn	20
C	120	Mo	10
Cd	0.4	Ni	10
Ca	20	N	15
Cl	100	O	700
Co	10	P	75
Cr	70	Pb	6
Cu	10	Na	25
Fe	130	Si	7
H	30	Ti	15
Hf	200	V	10

b) niobium (vacuum sintered), impurities :

Element	Content in ppm	Element	Content in ppm	Element	Content in ppm
Al	20	Hf	80	Si	100
B	1	Hg	20	Sn	20
C	30	Mn	20	Ta	300
Cd	5	Mo	20	Ti	150
Co	20	N	144	V	20
Cr	20	Ni	20	W	150
Cu	40	O	60	Zn	20
Fe	100	Pb	20	Zr	500

c) tin : purity 99.99 %

TABLE II

Chemical composition of the billets

Heat No.	Alloy	Sampling at the billet	Contents (weight-%)				
			Sn	Fe	Cr	Ni	Nb
10 431	Zircaloy-2	top	1.57	—	—	—	—
10 431	Zircaloy-2	bottom	1.38	0.095	0.084	0.054	—
10 433	Zircaloy-2	top	1.40	—	—	—	—
10 433	Zircaloy-2	bottom	1.62	0.11	0.089	0.061	—
10 435	ZrNb3Sn1	top	1.03	—	—	—	2.99
10 435	ZrNb3Sn1	bottom	1.02	—	—	—	2.96
10 437	ZrNb3Sn1	top	1.09	—	—	—	2.90
10 437	ZrNb3Sn1	bottom	1.08	—	—	—	2.78
Nominal values :	Zircaloy-2		1.2-1.7	0.1	0.1	0.06	—
				$Fe + Cr + Ni = 0.18 - 0.38$			
Nominal values :	ZrNb3Sn1		1.0				3.0

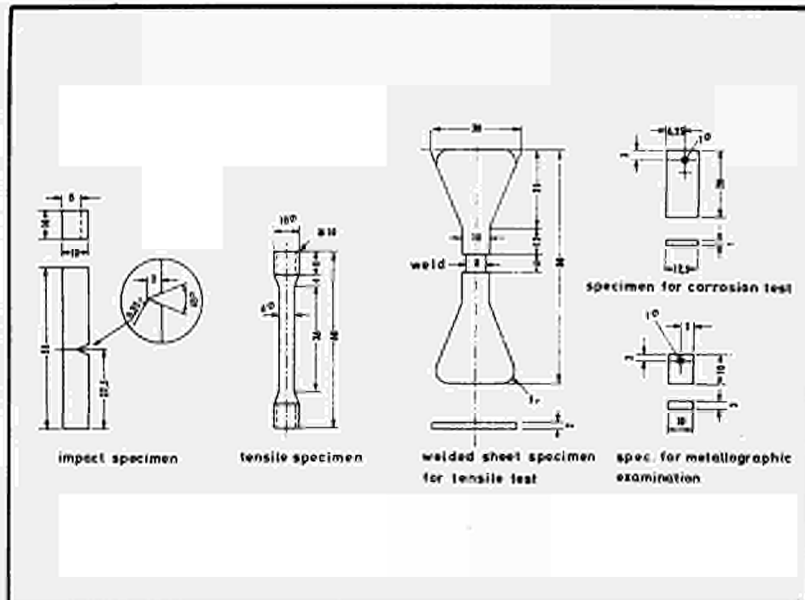


FIG. 4 — Dimensions of specimens for the irradiation tests.

TABLE III
Fabrication and heat-treatment of both alloys

Breakdown of the cast structure	Hot rolling	Cold work	Final treatment	Destination of the specimens
Extrusion at 800°-850° C/anneal (Zircaloy-2: 1 h 650° C/air ZrNb3Sn1 : 1 h 750° C/furnace)	—	28 % cold swaged	Zircaloy-2 : 1 h 650° C/air ZrNb3Sn1 : 16 h 580° C/air	Cylindrical tensile specimens (both alloys)
Forging down to plates, 30 mm thickness, at abt. 850° C/ removal of scale	—	15 %-20 % coldrolled/anneal (Zircaloy-2 : 1 h 650° C/air ZrNb3Sn1 : 1 h 760° C/furnace/), coldrolled to 11 mm	Similar	Impact specimens (both alloys)
		Coldrolled to 2 mm	Similar	Sheet specimens for tensile test with welds (both alloys)
		Coldrolled to 1 mm	Similar	Specimens for microscopic examinations and for corrosion tests («cold rolled», both alloys)
	At abt. 800° C hot rolled to 3 mm/ removal of scale	50 % coldrolled to 1 mm	Similar	Corrosion samples (« hot and cold rolled », both alloys)
		β -anneal 1 h 1000° C/air, 50 % coldrolled to 1 mm	Similar	Corrosion samples « β -annealed » (ZrNb3Sn1)

The final heat-treatment of zircaloy-2 was 1 hr at 650° C. Fig. 5a is a microsection of a finally annealed cylindrical tensile specimen, the structure of which consists of recrystallized α -grains superimposed on a network of intermetallic stringers originating from the extrusion. Microsections of the « cold rolled » and « hot and cold rolled » corrosion samples after final heat-treatment are shown in Fig. 5b and 5c.

The corrosion resistance of ZrNb3Sn1 is heavily affected by the final anneal, similarly to binary ZrNb alloys. Prior investigations ⁽¹⁵⁾ proved the necessity of an anneal below the α/β -transformation range, i.e. below 590° C. The ZrNb3Sn1 material has therefore been finally heat-treated 16 hr at 580° C.

Fig. 6a is a microsection taken from a cylindrical tensile specimen after the optimal heat-treatment below the monotectoid temperature. The dark regions imbedded in the

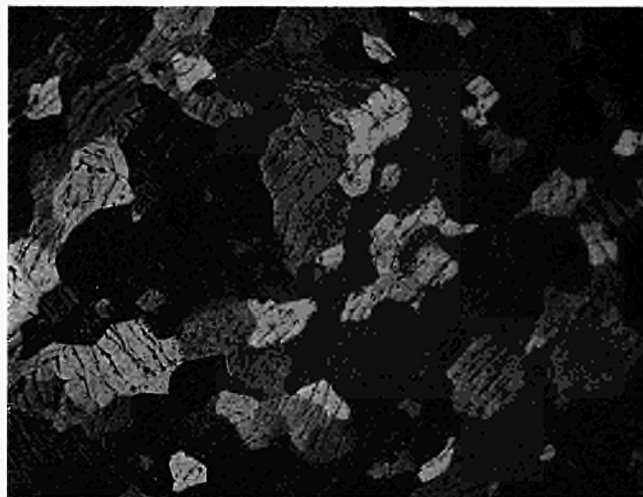


FIG. 5a — Zircaloy-2, annealed cylindrical tensile specimen; polarized light; $\times 300$.

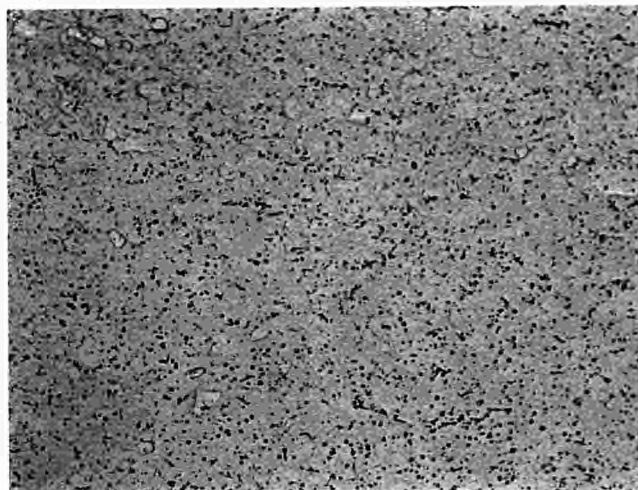


FIG. 5b — Zircaloy-2, cold rolled sheet; $\times 300$.



FIG. 5c — Zircaloy-2, hot and cold rolled sheet; $\times 300$.

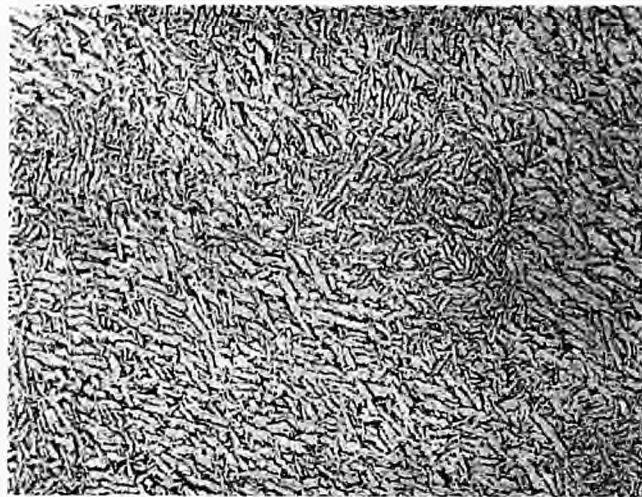


FIG. 6a — ZrNb₃Sn₁, cylindrical tensile specimen after 580° C-anneal; × 300.

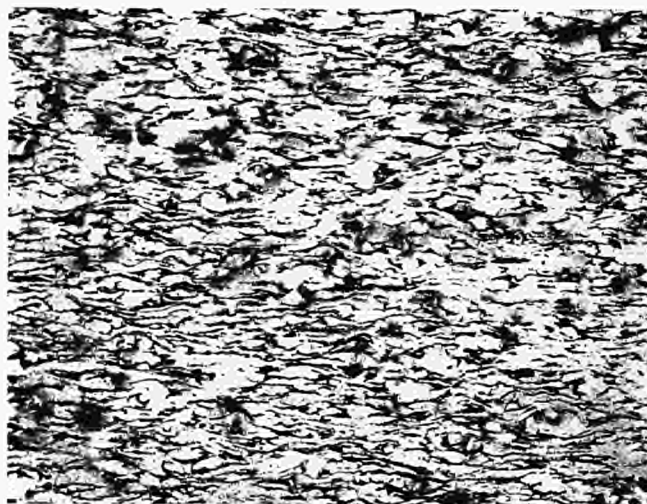


FIG. 6b — ZrNb₃Sn₁, cold rolled sheet; × 300.

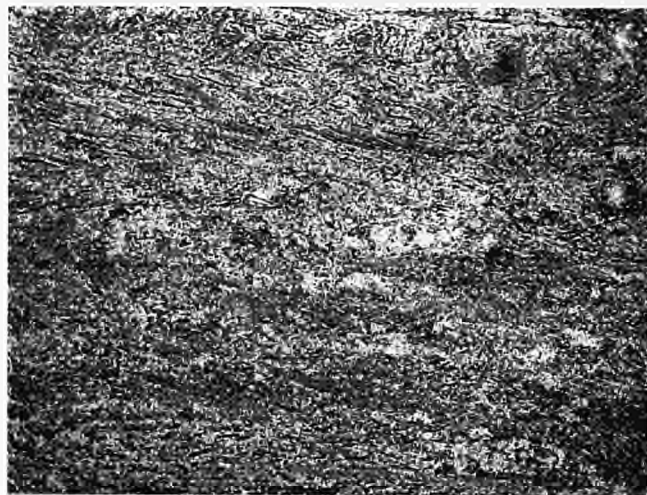


FIG. 6c — ZrNb₃Sn₁, hot and cold rolled sheet; × 300.

α_{Zr} -structure are accumulations of finely dispersed precipitates of β_{Nb} . Contrary to Fig. 6a and to the « cold rolled » structure of the 1 mm sheet (Fig. 6b), the β_{Nb} -precipitates of the « hot and cold rolled » structure (Fig. 6c) are rather homogeneously dispersed. The β -anneal before the last cold work leads to a similar but coarser structure as shown in Fig. 6c.

The dimensions of the specimens used for this investigation are shown in Fig. 4. The flat tensile specimens were welded without filler material in an evacuated, argon-filled chamber. After the welding procedure, a repetition of the 580° C-anneal was necessary to improve the corrosion resistance of the weld (19). The cross section of the specimens was reduced in the weld to predetermine the most probable location of the fracture.

For this investigation the Izod type impact specimens were chosen thus enabling us to compare the measured impact strength with literature data for zirconium and zircaloy-2. It is known that in metals with hexagonal lattice, the impact strength varies remarkably at different orientations to the rolling direction. In a *preliminary experiment*, impact specimens were taken from a zirconium plate in the four main orientations.

- a) notch in rolling plane and rolling direction (TH);
- b) notch in rolling plane and vertical to rolling direction (LH);
- c) notch vertical to rolling plane, specimen parallel to rolling direction (LV);
- d) notch vertical to rolling plane, specimen transverse to rolling direction (TV).

Fig. 7 shows the effect of texture and temperature on the impact strength. Notches in vertical position to rolling plane give lower impact values than horizontal positions. The lowest impact strength is obtained when specimens are taken transverse to rolling direction (notch in rolling direction, like under a). This corresponds to the results of Adam-

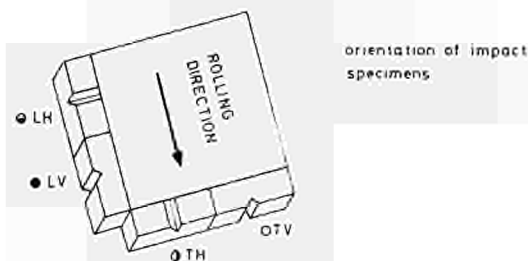
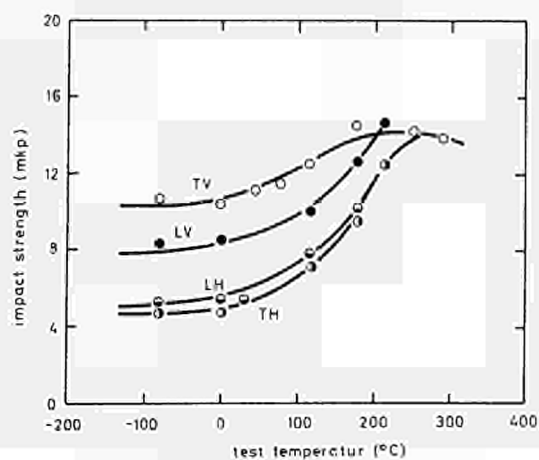


FIG. 7 — Impact energy curves for various specimen orientations of zirconium

son *et al.* ⁽²³⁾. This position was chosen for the irradiation experiments, since notches oriented in such a way on reactor-components easily tend to cause fractures.

3.2 — Irradiation Experiments

The irradiation program was realized in the swimmingpool reactor FRG-1 (Geesthacht-Tesperhude, Germany). The program included two different test series :

a) Irradiation of tensile specimens

The specimens were mounted in open containers according to Fig. 8, contacting the pool water (temp. abt. 45° C) during the irradiation. The two inserted frames enabled a withdrawal of the specimens. The upper frame was withdrawn after receiving about one third of the integrated fast flux (*) applied to the second frame. One of the containers was irradiated in a peripheral position of the reactor, a second container in a central position of the reactor core.

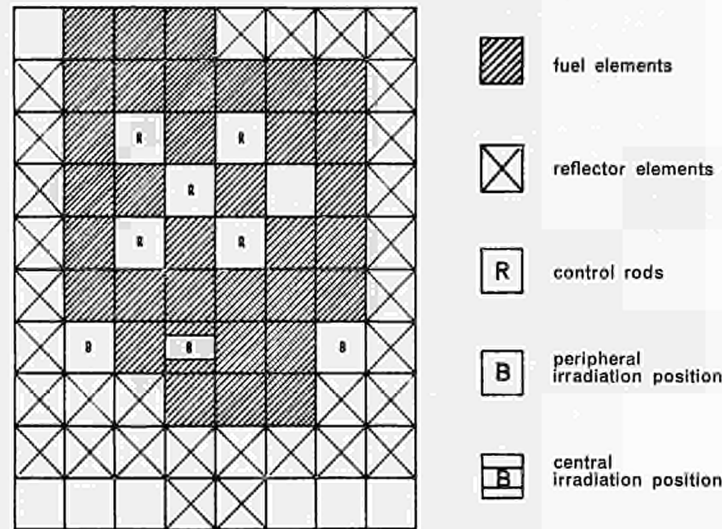


FIG. 8 — Positions of the specimen containers in the reactor FRG-1.

Here, the integrated flux of fast neutrons reached about twice the value of that in the peripheral position. Table IV contains the spectral distribution of the neutron fluxes in the two irradiation positions, measured at the medium height of the uranium zone at a reactor power of 5 MW.

b) Irradiation of samples under corrosion attack.

A sketch of a corrosion autoclave with safety capsule can be seen in Fig. 9. A detailed description of this autoclave was given in a prior publication ⁽²⁰⁾. The autoclaves were sealed by welding after the addition of a calculated quantity of deionized water under

(*) The "integrated fast flux" includes all neutrons with $E > 1$ MeV. This is the most effective part of the energy spectrum of neutrons, causing material damages.

TABLE IV

Spectral distribution of the neutron fluxes in two irradiation positions (medium height of the uranium zone, reactor power = 5 MW)

Irradiation position	Neutron fluxes ($n/cm^2 \cdot s$)			$\frac{\Phi \text{ fast}}{\Phi \text{ therm.}}$
	$\Phi \text{ therm.}$ ($E < 0.5 \text{ eV}$)	$\Phi \text{ epitherm.}$	$\Phi \text{ fast}$ ($E > 1 \text{ MeV}$)	
Periphery of the core . . .	$4.0 \cdot 10^{13}$	$2.3 \cdot 10^{12}$	$9.5 \cdot 10^{12}$	0.238
Center of the core	$4.7 \cdot 10^{13}$	$4.4 \cdot 10^{12}$	$2.4 \cdot 10^{13}$	0.512

He-atmosphere. Heated to the test temperature of 400° C, the steam pressure rose to 100 at. The γ -heating causes some problems, if the samples have no contact with the pool-water. The design of the capsule containing the autoclave took this into consideration. The maximum temperature in the center of the capsule at full reactor power was about 325° C. The difference from the desired temperature of 400° C was eliminated by additional electrical heating.

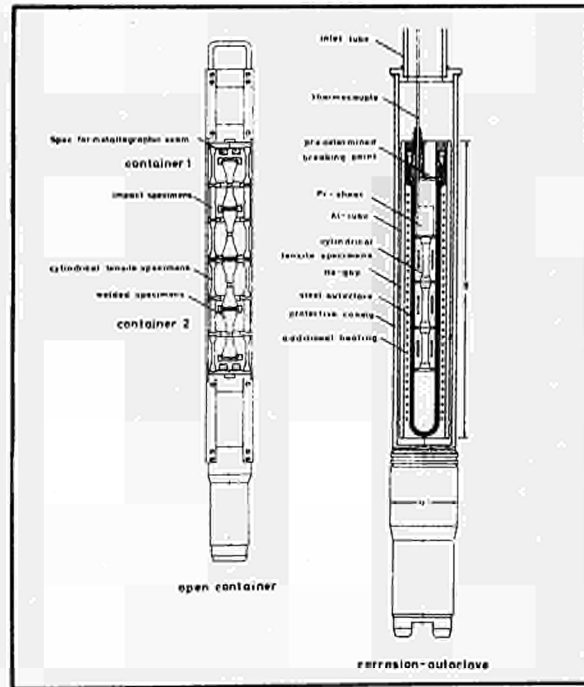


FIG. 9 — Capsules for irradiation experiments.

Two autoclaves with corrosion samples were irradiated in two peripheral positions up to integrated fluxes of

- 0.75·10¹⁹ fast n/cm^2 ($> 1 \text{ MeV}$)
- 2.4·10¹⁹ thermal n/cm^2 ($< 0.5 \text{ eV}$)

and

$1.5 \cdot 10^{19}$ fast n/cm^2 (> 1 MeV)

$4.8 \cdot 10^{19}$ thermal n/cm^2 (< 0.5 eV)

respectively. These integrated fluxes are correlated with exposure times of 401 and 817 hours.

Fig. 8 shows the arrangement in the reactor core and the positions of the capsules for tensile specimens and corrosion autoclaves. The left peripheral position was used for both an autoclave and an open container.

Since for zircaloy-2 the saturation of the irradiation strengthening is attained after integrated fast fluxes of about $1 \cdot 10^{20}$ n/cm^2 , we estimated an integrated fast flux of abt. $5 \cdot 10^{19}$ n/cm^2 to be sufficient for a comparison between the two alloys zircaloy-2 and ZrNb3Sn1. This assumption was justified by the results obtained.

The integrated thermal flux was measured with the reaction $^{59}\text{Co} (n, \gamma) ^{60}\text{Co}$ with the neutron capture cross-section $\sigma_0 = \sigma. (2200 \text{ m/s}) = 38$ barns and the half-life period of 5.2 years for ^{60}Co . The integrated fast flux could be measured with the reaction $^{54}\text{Fe} (n, p) ^{54}\text{Mn}$ with the activation cross section ($E > 1$ MeV) = 77 m barns. Since the half-life of ^{54}Mn (303 d) is of the same order as the irradiation periods, we had to take into account the reactor-standstill at the weekends. A second method using the reaction $^{58}\text{Ni} (n, p) ^{58}\text{Co}$ was applied, but on account of the different cross sections, we preferred the results of the iron detector measurements.

The Fe, Ni, and Co activation detectors (Fe and Ni covered with a 0.7 mm Cd-foil) for the open containers with tensile specimens were mounted in aluminium cans, replacing specimens. The detectors for the autoclaves could not be placed close to the specimens within the autoclaves. They were fixed outside the capsules, and the decrease of the thermal flux within the autoclaves was calculated to be 7.2 %. The calculation of the neutron fluxes from the detector activities was performed in applying the usual method (for example as described in ⁽²¹⁾).

3.3 — Examination of Irradiated Specimens

For these examinations, a concrete cell and some lead cells were available. Dismounting of the capsules, sawing up the autoclaves, examination of the tensile and impact specimens were executed in the concrete cell, the metallographic specimens and corroded samples were investigated in the lead cells.

For the tensile tests, a 5 t-tensile machine with remote control (« Testatron », Fa. Wolpert, Ludwigshafen) was used. The 0.2 %-offset yield strength was taken from the load elongation diagram, the elongation being magnified 34.4 times. The elongation and reduction of area were measured, using the optical part of a hardness tester for remote control. The hardness was determined on the impact specimens by a hardness tester remotely operated (« Frankoskop », Fa. Frank, Weinheim).

The hydrogen pickup of the corrosion specimens was determined by heating inductively to about 1400° C and evaluating the volume of the expelled H₂.

3.4 — Comparative Tests without Irradiation

Besides metallographic examinations, impact and tensile tests (specimens of Fig. 4), we investigated the effect of a water change on the corrosion behaviour.

During the irradiation experiments an exchange of the water in the autoclaves was not possible. It is known that the composition of steam can change remarkably due to radiolytic processes. Further complications are caused by the increased partial pressure of hydrogen in the autoclave due to corrosion processes and by the thermocycles according to the operation schedule of the reactor, all these environmental effects possibly influencing the corrosion rate. Therefore, two comparative tests in steam of 400° C were provided :

a) in a steel-autoclave (0.5 l volume) with removable cover, the water being frequently changed (on an average every three days); steam pressure 200 at.

b) in two steel-autoclaves (0.1 l volume), identical to the autoclaves used for the in-pile test, the cover being sealed by a weld. This test was executed without water exchange and in adopting the temperature cycles of the in-pile tests; steam pressure 100 at. One autoclave kept the temperature of 400° C for 401 hr, the other for 817 hr.

4 — Corrosion Behaviour under Irradiation

4.1 — Results

The *weight gains* after 401 hr and 817 hr in-pile corrosion are listed in Table V. The same table contains the weight gains measured during the two comparative tests without irradiation.

TABLE V
Weight gains and hydrogen uptake in 400° C steam with and without radiation

Experimental conditions	Alloy	Final material treatments ^a	Weight gains (mg/dm ²)		Hydrogen uptake (mg/dm ²)	
			Corr. time 401 hr	Corr. time 817 hr	Corr. time 401 hr	Corr. time 817 hr
Corrosion under radiation, in a sealed 0.1 l-autoclave, without water exchange	Zircaloy-2	c.r.	97 ^b ?	— 58 ^b	5.8	15.2
	Zircaloy-2	c.r.	—338 ^b	118 ^b	6.6	18.4
	Zircaloy-2	h.c.r.	124 ^b ?	123	8.1	8.0
	Zircaloy-2	h.c.r.	—263 ^b	^b	5.5	15.8
	ZrNb3Sn1	c.r.	210 ^b ?	501 ^b	4.1	33.4
	ZrNb3Sn1	c.r.	238 ^b ?	—137 ^b	4.9	31.2
	ZrNb3Sn1	h.c.r.	7.8 ^b	291 ^c	0.11	19.7
	ZrNb3Sn1	h.c.r.	84	305 ^c	2.3	21.2
	ZrNb3Sn1	β-a	76	295 ^b ?	2.4	22.0
Corrosion without irradiation in a 0.5 l-autoclave with frequent water exchange	Zircaloy-2	c.r.	30	33	0.20	0.45
	Zircaloy-2	h.c.r.	19	26	0.23	0.38
	ZrNb3Sn1	c.r.	45	56	0.22	0.70
	ZrNb3Sn1	h.c.r.	38	65	0.23	0.45
	ZrNb3Sn1	β-a.	38	54	0.25	0.60
Corrosion without irradiation in a sealed 0.1 l-autoclave, without water exchange	Zircaloy-2	c.r.	41	148	1.41	6.6
	Zircaloy-2	h.c.r.	179	121	1.7	4.4
	ZrNb3Sn1	c.r.	180	71	1.7	1.16
	ZrNb3Sn1	h.c.r.	38	88	1.66	1.88
	ZrNb3Sn1	β-a.	38	45	0.87	1.38

^a c.r. « cold-rolled »
h.c.r. « hot and cold rolled »
β-a. « β-annealed »
(compare Tab. III)

^b Parts of the oxide film already peeled off.
^c oxide film with small blisters.

The weight gains as a function of time during the *ex-reactor test* with frequent water exchange are shown in Fig. 10. The exponents of the corrosion function of both alloys are similar, but the absolute values of the total weight gain of ZrNb3Sn1, especially in the post transition region, are twice those of zircaloy-2. Some new results ⁽²⁴⁾ suggest that this difference may be eliminated by an improved final heat-treatment. The weight gains canning tubes treated in such a way and exemplified in Fig. 10 are remarkably lower and can compete with those of zircaloy-2. The influence of fabrication history is of second order in comparison with the influence of the final heat-treatment. In the pretransition range, the « cold rolled » material has the highest oxidation rate, the « hot and cold rolled » material the lowest one. After the transition point, these differences will disappear.

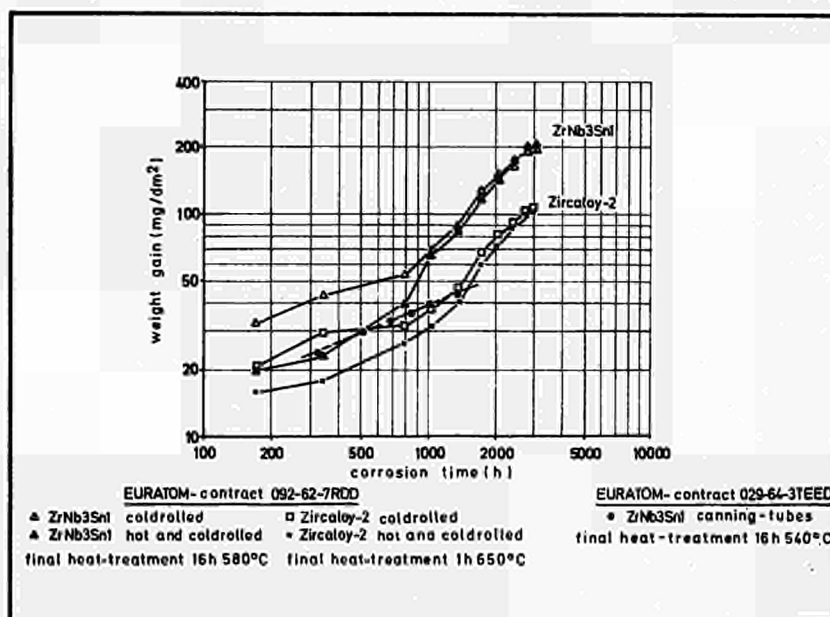


FIG. 10 — Weight gains of zircaloy-2 and ZrNb3Sn1 during steam-corrosion at 400° C (without irradiation, frequent water exchange).

During the *in-pile test* the oxidation was severely enhanced. The weight gains of different samples fluctuate within a wide range, which is partly due to the start of breakaway. The colour of the intact oxide film was dark gray. The peeled-off regions had a white or light-gray colour. The inclination of zircaloy-2 for peeling-off was somewhat higher than that of ZrNb3Sn1. Here, the breakaway had less advanced and was indicated only by small blisters. The acceleration of corrosion is not only caused by the radiation. This could be proved by comparative tests in sealed autoclaves without water exchange : after prolonged corrosion exposure the weight gains are in this test much higher than with frequent water exchange. For better comparison, an enhancement factor

$$f = \Delta W_1 / \Delta W_2 \text{ is defined,}$$

where ΔW_1 is the weight increase in the enhanced reaction, ΔW_2 the weight increase without enhancement during the same period. In Table VI, different enhancement factors are reported :

- a) enhancement of oxidation by omission of water exchange (comparison of the *ex-reactor tests* in the 0.1l- and 0.5 l-autoclaves; enhancement factors f_{W_3} and f_{W_4} after 401 hr and 817 hr oxidation).

The oxidation is enhanced with zircaloy-2 and — in a less explicit manner — with ZrNb3Sn1 in cold rolled condition;

- b) enhancement of oxidation by radiation (f_{w_1} , f_{w_2});
 comparison of the in-pile and ex-reactor tests in sealed autoclaves without water exchange. After 401 hr corrosion-time the oxidation of both alloys is somewhat enhanced ($f_{w_1} \approx 2$). After 817 hr, the enhancement, especially of ZrNb3Sn1 has increased. The figures for zircaloy-2 are unreliable because of the breakaway effects.
- c) enhancement of hydrogen uptake by omission of water exchange without irradiation (f_{H_3} , f_{H_4});
 the enhancement is considerable and increases with zircaloy-2 with a prolonged exposure ($f_{H_3} \approx 7$; $f_{H_4} \approx 13$), while it decreases with ZrNb3Sn1;
- d) enhancement of hydrogen uptake by radiation (f_{H_1} , f_{H_2});
 after 401 hr zircaloy-2 absorbed 4 times, ZrNb3Sn1 only approx. twice as much in comparison with the tests in sealed autoclaves. After 817 hr, f_{H_2} of zircaloy-2 is not well established; f_{H_2} of ZrNb3Sn1 is very high, causing total hydrogen contents of 700 to 1200 ppm.

TABLE VI

Enhancement of oxidation in sealed autoclaves with and without radiation

Definition of enhancement	Alloy	Final material treatments ^a	Enhancement of oxidation		Enhancement of hydrogen uptake	
			f_w after 401 hr	f_w after 817 hr	f_H after 401 hr	f_H after 817 hr
Enhancement in the corrosion tests under radiation as against the test in sealed autoclaves without radiation	Zircaloy-2	c.r.	>2	?	4.4	2.5
	Zircaloy-2	h.c.r.	$\approx 1?$	>1	4.0	2/-36
	ZrNb3Sn1	c.r.	>1.2	>7	2.7	17.2
	ZrNb3Sn1	h.c.r.	2.2	3.4	0.7	10.9
	ZrNb3Sn1	β -a.	2	>6	2.7	16.0
Enhancement in the corrosion tests without radiation in sealed autoclave as against the test in the 0.5-l autoclave (frequent water exchange)	Zircaloy-2	c.r.	1.4	4.5	7.0	14.7
	Zircaloy-2	h.c.r.	9.4	>4.7	7.4	11.6
	ZrNb3Sn1	c.r.	4.0	>1.3	7.7	1.7
	ZrNb3Sn1	h.c.r.	1.0	1.4	7.2	4.2
	ZrNb3Sn1	β -a.	1.0	0.8	3.5	2.3

^a Explanation : see Table V.

The values fluctuate too much to establish differences with different material treatments. Fairly well established are the following results :

- a) omission of water exchange causes an enhancement of the oxidation of zircaloy-2 and a much higher enhancement of hydrogen absorption of both alloys.
- b) the enhancement of oxidation by radiation is not so well established. After a prolonged exposure, some acceleration of oxidation is noticed at least with the ZrNb3Sn1-samples

($f_{w_2} \approx 3.4-7$). The hydrogen absorption of ZrNb3Sn1 is increased to a detrimental level. The figures for zircaloy-2 are scattering, but also with zircaloy-2 some enhancement is observed.

The *microscopic examinations* of the irradiated corrosion specimens could not prove any structural change due to irradiation damages. It is known that the hydrogen, originating from the reduction of steam on the zirconium surface, is partially absorbed by the material and will nucleate in precipitates of zirconium-hydride. This nucleation takes place when the material is cooled down from the corrosion temperature, undercutting the maximum solution of hydrogen in α -zirconium. The hydride phase precipitates at the grain boundaries and in the α -grains in the form of small platelets. The internal stresses caused by the last steps of cold work influence the orientation and distribution of these platelets. The platelets are supposed to line up parallel to the internal stresses (⁵⁷). This stress-hypothesis cannot explain every detail of the phenomena observed. The sheet investigated in this case has been finally recrystallized and should be free of residual stresses. Therefore, random distributions of the orientation of hydride-precipitates should be expected. The dark thread-like structures visible in Figs. 12-13 are the rows of lined-up precipitates, the precipitates themselves being too small to be visible individually.

The hydrides are generally oriented in the rolling direction of the sheet. This general orientation is not changed by the irradiation. Also after 817 hr of in-pile and out-pile corrosion, the orientation parallel to the sheet surface still exists. In conformity with the results of the hydrogen analysis less hydrides are visible in the samples corroded without irradiation. The in-pile corroded samples contain a much higher amount of hydrides after 817 hr corrosion than after 401 hr.

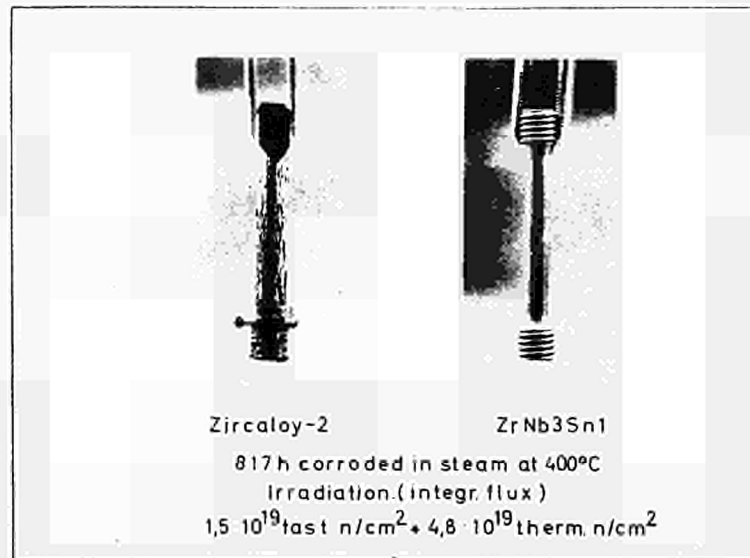
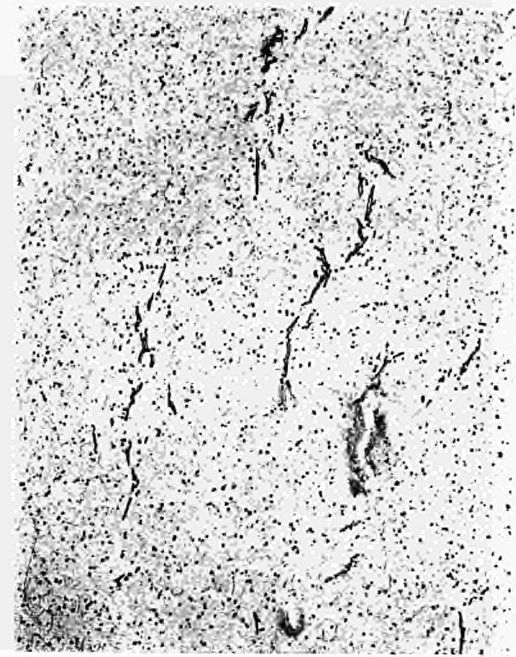
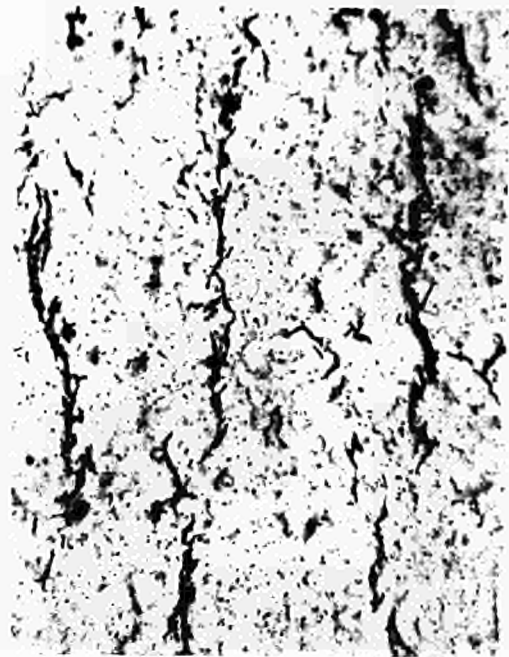


FIG. 11 — Tensile specimens after in-pile corrosion (817 hr 400° C).

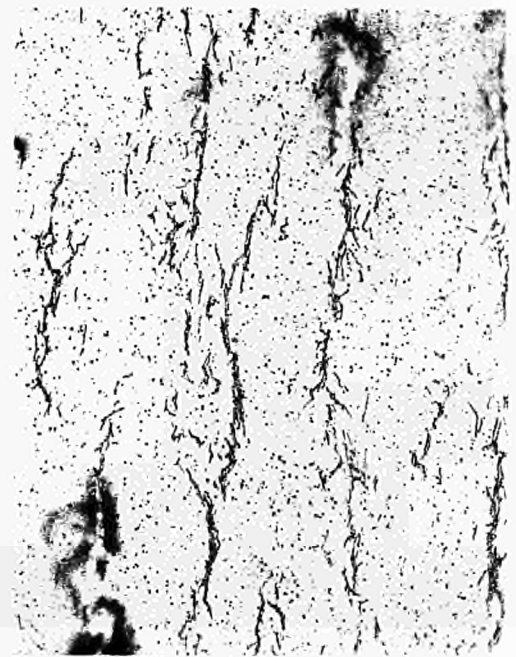
The *mechanical properties after radiation-enhanced corrosion* are very important for the technical application of zirconium alloys. The cylindrical tensile specimens for this test have likewise been corroded in the sealed autoclaves. Fig. 11 gives an impression of the appearance after corrosion under radiation. The zircaloy-2 specimen exhibited after 817 hr of exposure detrimental corrosion effects; the breakaway had already started. The ZrNb3Sn1 specimens were less attacked by corrosion. Fig. 14 shows the mechanical pro-



a



c



b



d

FIG. 12a — Zircaloy-2 sheet after 492 hr corrosion in 400° C-steam without irradiation; $\times 300$.
FIG. 12b — Zircaloy-2 sheet after 817 hr corrosion in 400° C-steam without irradiation; $\times 300$.
FIG. 12c — Zircaloy-2 sheet after 401 hr corrosion in 400° C-steam with irradiation (integr. flux : 0.75×10^{19} fast $n/cm^2 + 4.4 \times 10^{19}$ thermal n/cm^2); $\times 300$.
FIG. 12d — Zircaloy-2 sheet after 817 hr corrosion in 400° C-steam with irradiation (integr. flux : 1.5×10^{19} fast $n/cm^2 \times 4.8 \times 10^{19}$ thermal n/cm^2); $\times 300$.



a



c



b



d

FIG. 13a — ZrNb₃Sn₁ sheet after 492 hr corrosion in 400° C-steam without irradiation; × 300.

FIG. 13b — ZrNb₃Sn₁ sheet after 817 hr corrosion in 400° C-steam without irradiation; × 300.

FIG. 13c — ZrNb₃Sn₁ sheet after 401 hr corrosion in 400° C-steam with irradiation (integr. flux : 0.75×10^{19} fast $n/cm^2 + 4.4 \times 10^{19}$ thermal n/cm^2); × 300.

FIG. 13d — ZrNb₃Sn₁ sheet after 817 hr corrosion in 400° C-steam with irradiation (integr. flux : 1.5×10^{19} fast $n/cm^2 + 4.8 \times 10^{19}$ thermal n/cm^2); × 300.

erties as a function of corrosion and irradiation time. The plot also contains values of specimens corroded without irradiation in the sealed autoclaves (without water exchange). After 401 hr corrosion time, the differences between irradiated and unirradiated specimens are very small. After 817 hr the ultimate tensile strength and the yield strength of ZrNb3Sn1 have increased, whilst the reduction in area and elongation are insignificantly reduced. Zircaloy-2 was too heavily corroded to be tested.

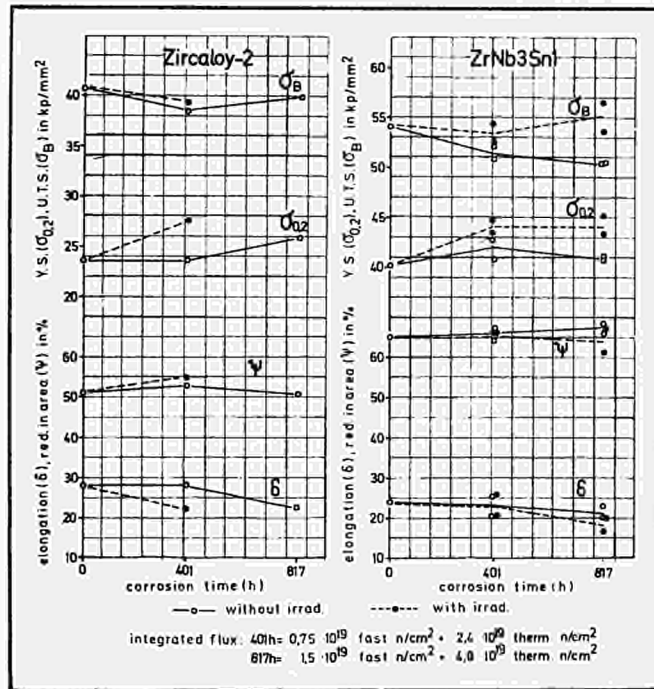


FIG. 14 — Mechanical properties of zircaloy-2 and ZrNb3Sn1 after steam-corrosion with and without irradiation.

4.2 — Discussion

During the last years the influence of irradiation on the corrosion of zircaloy and ZrNb-alloys in water and steam has been discussed by several authors (25,35). The statements concerning the factor of enhancement by irradiation are contradictory. Several authors suggest remarkable enhancements of corrosion : Krenz (26), for instance, a factor 2, Nelson (32) a factor 4.3 whereas Maffei (36) stated with PRTR zircaloy-2 tubes an enhancement factor of 5, and Burns (31) measured in a low oxygen water loop at 280° C an enhancement by a factor of up to 10 during the corrosion of zircaloy and ZrNb3Sn1 specimens. Asher *et al.* (27, 28, 35) investigated the corrosion of zircaloy-2 and ZrNb2. 5 in steam. The weight increase has been enhanced eight-fold by *n*-radiation in the temperature range of 300-340° C. At 400 and 450° C, the enhancement had disappeared. The most famous example of corrosion without enhancement by radiation are the blanket elements in the Shippingport-PWR (32). McClintock (37) noticed no radiation influence in water with small H₃BO₃ additions. These contradictory results confirm the opinion of Cox (25) that enhancement of corrosion is frequently caused by environmental effects, like impurities in the coolant, and not only by radiation itself.

Our results demonstrate the heavy influence of environment. Only the omission of water exchange causes an enhancement of oxidation by a factor of up to five, especially

in the post-transition region (817 hr). This observation is in conformity with the results of Flint (38). He attributes the lower weight gains in fresh water to a certain solubility of ZrO_2 in H_2O . Since we noticed also a heavy enhancement of the hydrogen uptake, this hypothesis cannot explain our results. The following environmental effects have to be discussed :

- a) thermocycling during corrosion test; as mentioned in chap. 3.4, the test temperature has been adapted to the reactor cycles. However, according to previous studies (39, 40), thermal cycling has no influence on the oxidation of zircaloy-2;
- b) impurities contaminating the steam or the metal surfaces; the increase of the conductivity of water during corrosion indicates some ionic contamination. Gaseous impurities (O_2 , CO_2 , N_2) are neglectable, since the autoclaves have been filled and welded under He-atmosphere.
- c) increased partial pressure of hydrogen in the steam, originating from the reduction of water and the only partial absorption of hydrogen by the corrosion specimens.

Previous investigations (40) did not reveal any influence of the hydrogen pressure on oxidation. Yet, the increased hydrogen uptake might be caused by the increasing hydrogen pressure, since also molecular hydrogen can be cracked and absorbed at zirconium surfaces. An additional increase of oxidation caused by the enhanced hydrogen uptake might be due to the structure and conduct of the oxide film being affected by the neighbouring metal that contains an increasing amount of absorbed hydrogen. Ambler (58) observed a brittle-ductile transition on Zr-hydride layers between 40 and 80° C. During the temperature cycles the corroded samples crossed this transition range several times. The formation of cracks on the oxide metal interface might accelerate the crack formation in the oxide film.

During the irradiation test the hydrogen uptake is enhanced very substantially (factors of up to 36, increasing by exponential law). It is quite possible that the partial pressure of hydrogen in the autoclaves was additionally increased by radiolytic decomposition. We are inclined to assume that the increased hydrogen uptake is not so much caused by radiation damage, but rather by the high hydrogen content of the steam. The hydride formation (orientation and distribution) is apparently not influenced by radiation.

The enhancement factors of oxidation during irradiation are not so well established due to some oxide spalling (especially zircaloy-2 !). However there is no doubting the existence of some enhancement : the weight gains of ZrNb3Sn1 have increased two-fold after 401 hr and up to seven-fold after 817 h. The breakaway of ZrNb3Sn1 seems to be deferred as compared with zircaloy-2. Asher (35) reports that at 400° C no enhancement of corrosion is to be expected, since the radiation damages which, in his opinion, cause the increase, will recover at 400° C. Analogously to the unirradiated test, the enhancement of oxidation might be discussed in terms of the increased hydrogen absorption.

The mechanical properties are not influenced very much by the corrosion under radiation. The strengthening effect of radiation disappears at 400° C due to recovery (comp. chap. 6). The increased hydrogen absorption causes only slight reductions of elongation because of the large cross section of the cylindrical specimens. To thinwalled canning tubes the observed hydrogen uptake would be detrimental.

5 — Mechanical Properties after Irradiation

5.1 — Results

Tensile tests have been performed at room-temperature, 300 and 450° C. Fig. 15 shows the yield strength ($\sigma_{0.2}$), the ultimate tensile strength (σ_B), the elongation (δ), and the reduction in area (Ψ) as a function of the test temperature and the integrated flux. At room-temperature, the yield strength of the zircaloy-2 specimens without irradiation was 23.5 kp/mm², increasing to 35.3 kp/mm² after $1.1 \cdot 10^{19}$ n/cm² and to 39.5 kp/mm² after $5.4 \cdot 10^{19}$ n/cm². This strengthening effect of irradiation is far less distinct with σ_B . While the elongation is decreased by irradiation, the reduction of area remains nearly unchanged. The strength of ZrNb3Sn1 without irradiation is more elevated ($\sigma_{0.2} = 40.2$ kp/mm²). The yield strength of this alloy is affected by the irradiation in the same way as that of zircaloy-2. The influence on the ultimate strength seems to be slightly higher. The elongation diminishes with higher fluxes, and the reduction in area also shows some decrease.

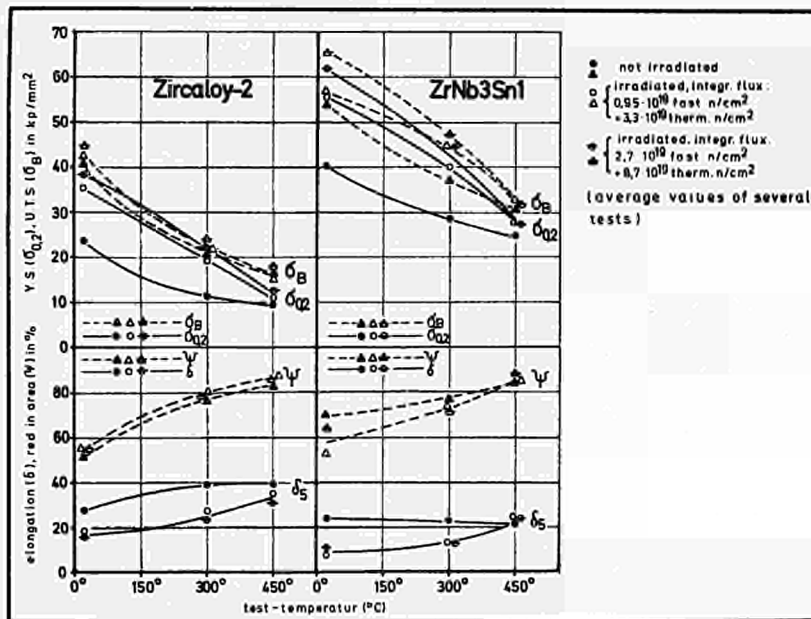


FIG. 15 — Influence of irradiation on the mechanical properties of zircaloy-2 and ZrNb3Sn1.

At elevated temperatures, the influence of irradiation will decrease due to some annealing process during the test performance. At 450° C no influence of the irradiation could be established.

According to the four irradiation intervals we can compare the influence of four different neutron fluxes. The influence of the thermal neutrons on the material properties is generally considered neglectable as compared with the influence of fast neutrons. Therefore, in spite of the different thermal fluxes, there is some reason to plot the mechanical properties at room-temperature and 300° C versus the fast integrated fluxes (Fig. 16). As already described, σ_B and $\sigma_{0.2}$ increased with irradiation, while δ decreased. The absolute change of the values is greater with ZrNb3Sn1 than with zircaloy-2 at both temperatures. The plot demonstrates the existence of a saturation value which is reached after a fast integrated flux of about $3 \cdot 10^{19}$ n/cm².

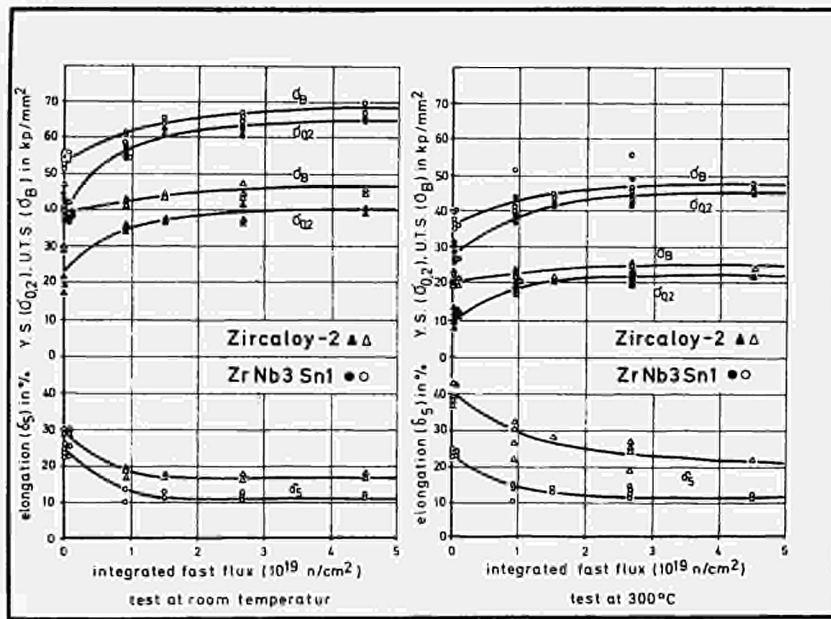


FIG. 16 — Effect of integrated fast flux on the mechanical properties.

The *impact values* at room-temperature have been determined in the unirradiated as well as in the irradiated stage. In addition, the influence of a heat-treatment at 300 and 360° C after irradiation has been investigated. Fig. 17 shows the impact strengths of samples of both alloys after different treatments. Zircaloy-2 exhibits a very slight decrease of impact values after prolonged irradiation; ZrNb3Sn1, on the other hand, exhibits a peak of impact strength with an integrated fast flux of $0.95 \cdot 10^{19} \text{ n/cm}^2$. The heat treatment is affecting the ZrNb3Sn1-alloy in some peculiar way, but the impact strength of zircaloy-2

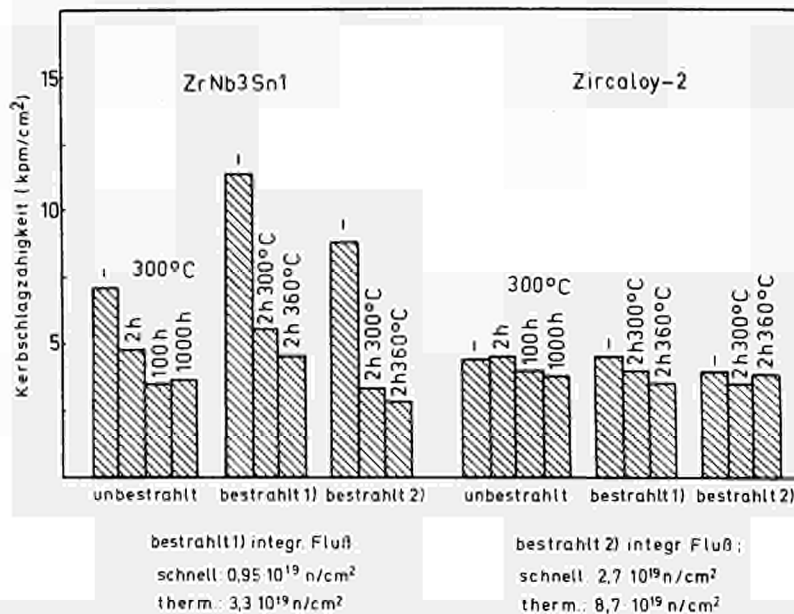


FIG. 17 — Effect of irradiation and additional heat-treatment on impact strength.

before and after irradiation is influenced by the heat-treatment only very slightly. The annealing treatment reduces the impact values of ZrNb3Sn1; a prolongation of the anneal and a rise of the temperature enhance this effect.

An examination of the *welded samples* proved that the effect on the ultimate strength was identical to that with the unwelded material. Fig. 18 indicates the strength after exposure to two different neutron fluxes depending on the test temperature. For comparison, the tendencies of Fig. 15 relating to the unwelded material are included. The strength of the welded samples is slightly higher than that of comparable unwelded material. This might be explained by some interstitial hardening caused by gas-absorption during the welding operations.

At the test temperature of 450° C, no influence of irradiation is left, while the strengthening effect of the weld-operation, especially with ZrNb3Sn1, is still evident.

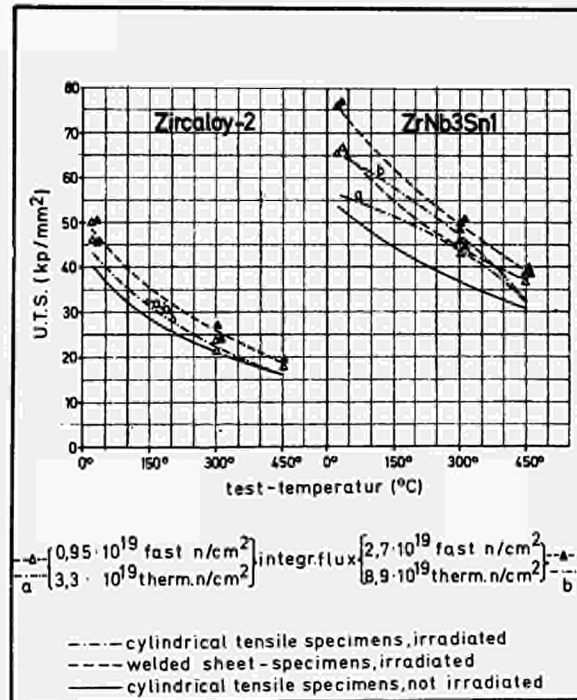


FIG. 18 — Ultimate tensile strength of welded sheet specimens after irradiation.

5.2 — Discussion

A number of investigations concerning the influence of fast neutrons on the *mechanical properties* of zircaloy have been published (41-51, 50). ZrNb2.5 was also the subject of irradiation studies (52, 53, 61).

On the whole, the investigations lead to the same results : irradiation increases the yield strength and the ultimate tensile strength. Similarly to strain-hardening, the increase of yield strength exceeds that of the ultimate tensile strength. The gain of yield strength observed by us at room-temperature after an irradiation of $4.5 \cdot 10^{19}$ fast n/cm^2 runs up to 70 % for zircaloy-2 and to 60 % for ZrNb3Sn1. Howe (45), for example, reported an increase of $\sigma_{0,2}$ of 55 % for annealed material, Scott (49) of 56 % at integrated fluxes of $> 10^{20} n/\text{cm}^2$. The in-pile temperatures have been elevated (280° C), therefore, a partial recovery probably occurring already at that temperature, explains the lower increases of yield strength. Ells

and Fidleris ⁽⁶¹⁾ recently stated yield strength changes of up to 80 % with ZrNb2.5 after irradiation to $3 \cdot 10^{19}$ n/cm^2 . The ultimate tensile strength is less influenced, the total increase noticed by us being 10 % for zircaloy-2 and 25 % for ZrNb3Sn1. This is in conformity with the previous results. The strengthening mechanism will not be discussed here. The radiation-induced defects act as additional pinning points for dislocations (detailed discussion: ⁽⁶¹⁾). The loss of total elongation, plotted in Figs. 15, 16, is due to the loss of uniform elongation (a similar effect known to be caused by strain-hardening ⁽⁵⁴⁾). The reduction in area remains unchanged during irradiation, thus indicating a good ductility in the irradiated stage.

The strengthening effect reaches a saturation value after about $3 \cdot 10^{19}$ n/cm^2 . The existence of this saturation has been frequently reported. The fast integrated fluxes, sufficient for this saturation fluctuate between 10^{19} and $5 \cdot 10^{20}$ n/cm^2 . These fluctuations may originate in the different neutron spectrums, in difficulties regarding exact flux-measurements, in different definitions of «fast» neutrons (> 500 eV or > 1 MeV), and in different irradiation temperatures. The saturation value is attained when the formation of new defects and the immediate recovery are in equilibrium.

The welded specimens underwent similar changes of tensile strength as the unwelded material.

The interpretation of the impact strength is only hypothetical. Our results concerning zircaloy-2 are in conformity with other reports ^(45, 52), denying a significant change of impact strength by neutron radiation. A recently published investigation ⁽⁶⁰⁾ leads to different conclusions showing impaired impact properties after irradiation. But this is only true at elevated test temperatures, while at room temperature the impact strength remains nearly unchanged. Contrary to zircaloy-2, the impact strength of ZrNb3Sn1 is increased substantially. It may be that this is due to precipitation hardening. The decreasing solubility of niobium in the α -phase possibly causes the clustering of Nb-atoms during cooling from 580° C. These clusters are destroyed by irradiation, but may reform during a 300° C-anneal. The excess vacancies caused by irradiation should accelerate this reformation.

6 — Investigation of Recovery

6.1 — Results

Specimens, irradiated with integrated fast fluxes of $0.95 \cdot 10^{19}$ and $2.7 \cdot 10^{19}$ n/cm^2 were annealed after irradiation for 2 hr at 300, 360 and 400° C. The mechanical properties at room-temperature after the anneal are plotted in Fig. 19. Up to 300° C the mechanical properties remain unchanged. However, annealing at 360 and 400° C caused a drop of $\sigma_{0.2}$ and a small increase of the elongation with both alloys. On an average, σ_B and Ψ remain unchanged. The recovery of $\sigma_{0.2}$ and δ is only a partial one, three quarters of the increase of $\sigma_{0.2}$ and decrease of δ caused by irradiation being still efficient after a 2 hr-anneal at 400° C.

Another criterion for the recovery phenomena at elevated temperatures are the differences $\Delta \sigma_B$, $\Delta \sigma_{0.2}$, $\Delta \delta$, $\Delta \Psi$ between the tensile values of the irradiated and unirradiated specimens, measured at 20, 300, and 450° C. These differences are likewise plotted in Fig. 19. The Δ -values at room-temperature symbolize the irradiation effect. At higher test temperatures, especially 450° C, the Δ -values decrease. This decrease demonstrates that the influences of recovery become already effective during the short anneal, in connection with the procedure of the tensile tests. Contrary to the merely partial recovery during isothermal

anneals as mentioned before, the strengthening effect of irradiation disappears completely during the 450° C-test.

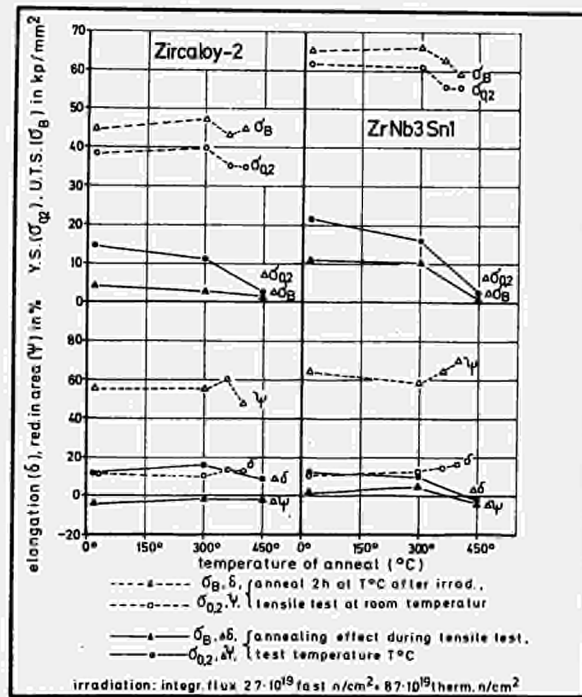


FIG. 19 — The recovery of irradiation damage as a function of temperature.

6.2 — Discussion

According to our results, no recovery of radiation damages is caused by after-irradiation anneals at 300° C. On the other hand, Howe^(43, 45) stated at 300° C a 50 %-regress of radiation-hardening. Similarly to a research conducted with ZrNb2.5 by Cupp⁽⁵³⁾ we noticed a recovery only at 360 and 400° C. The 1/2 h-anneal, in combination with the tensile tests at 450° C, resulted in a total recovery of radiation hardening.

REFERENCES

- 1 EURATOM-contracts Nos. 009-60-4 RDA, 047-61-4 RDA, 092-62-7 RDD (this investigation), 019-63-11 TEED, 029-64-3 TEED.
- 2 *Symposia on economic comparison of zirconium and stainless steel in nuclear power reactors*, New York, Febr. 13, 1958; Pittsburgh, March 11, 1958.
- 3 R. S. AMBARTSUMYAN, A. A. KISELEV, R. V. GREBENNIKOV, V. A. MYSHKIN, L. J. TSUPRUN and A. F. NIKULINA — *Proc. 2nd Intern. Conf. Atom. Energy Geneva*, 5 : 12 (1958).
- 4 O. S. IVANOV and V. K. GRIGOROVICH — *Proc. 2nd Intern. Conf. Atom. Energy Geneva*, 5 : 34 (1958).
- 5 V. S. EMELYANOV, Y. G. GODIN, A. I. EVSTYUKHIN — *Proc. 2nd Intern. Conf. Atom. Energy Geneva*, 5 : 69 (1958).
- 6 A. D. SCHWOPE, L. L. MARSH and W. CHUBB — *Report BMI-79* (1951).

- 7 A. D. SCHWOPE and W. CHUBB — *Report BMI-718* (1952).
- 8 F. B. LITTON — *Iron Age*, **167** (1951), No. 14, p. 95.
- 9 A. D. SCHWOPE and W. CHUBB — *J. Metals*, **4** : 1138 (1952).
- 10 US-Patent 2784084 (March 5, 1957).
- 11 F. B. LITTON and S. C. OGBURN — *Report AF-TR -59* (1954).
- 12 J. H. KEELER — *Report SO-2525* (1956).
- 13 W. CHUBB — *Trans. ASM*, **48** : 804 (1956).
- 14 K. ANDERKO, W. JUNG-KÖNIG, H. RICHTER, P. WINCIERZ, U. ZWICKER, K. SAGEL and R. ZIMMERMANN — 4. *Vierteljahresbericht vom 17. 4. 1961*, EURATOM-contract No. 009-60-4 RDD.
- 15 K. ANDERKO, W. JUNG-KÖNIG, H. RICHTER, H.-W. SCHLEICHER and U. ZWICKER — *Z. Metallkunde*, **53** : 503 (1962).
- 16 W. JUNG-KÖNIG, H. RICHTER and U. ZWICKER — *Metall*, **17** : 1 (1963).
- 17 W. JUNG-KÖNIG, H. RICHTER, J. C. TVERBERG, P. WINCIERZ and U. ZWICKER — *Report EUR 86.d* (1963).
- 18 H. RICHTER, P. WINCIERZ, K. ANDERKO and ZWICKER — *J. Less-Common Metals*, **4** : 252 (1962).
- 19 H. RICHTER and J. C. TVERBERG — *Metall*, **17** : 678 (1963); *Report EUR 1319.d* (1964).
- 20 J. AHLF, E. FISCHER, H. RICHTER and W. SPALTHOFF — *Kerntechnik, Isotopentechnik und -chemie*, **6** : 512 (1964).
- 21 D. ALBERT and K. FÄHRMANN — *Kernenergie*, **4** : 753 (1961).
- 22 W. JUNG-KÖNIG, H. RICHTER, W. SPALTHOFF, E. STARKE — *Atomkernenergie*, **11** : 47 (1966).
- 23 G. M. ADAMSON jr., J. O. BETTERTON jr., J. H. FRYE jr. and M. L. PICKLESIMMER — *Proc. 2nd Intern. Conf. Atom. Energy Geneva*, **5** : 3 (1958).
- 24 W. RUCKDESCHEL and H. RICHTER — 6. *Vierteljahresbericht vom 20. 6. 1966*, EURATOM-Contract No. 029-64-3 TEED.
- 25 B. COX — *Canad. Report AECL-2257*, May 1965.
- 26 F. H. KRENZ — *Intern. Congr. on Metallic Corr.*, London 1961.
- 27 R. C. ASHER, B. COX and J. K. DAWSON — *Intern. Atomic Energy Authority Symp. on Power Reactors*, Vienna 1961.
- 28 J. K. DAWSON, R. C. ASHER, J. BOULTON, B. WATKINS and J. N. WANKLYN — « The Properties of Zr-Alloys for Use in Water-Cooled Reactors ». *Proc. 3rd Intern. Conf. Atomic Energy, Geneva*, **9** : 461 (1964).
- 29 W. A. BURNS and H. P. MAFFEI — *USAEC Report HW-SA-3168* (1963).
- 30 W. A. BURNS and H. P. MAFFEI — *USAEC Report HW-82651* (1964).
- 31 W. A. BURNS — *USAEC-Report HW-84281*.
- 32 R. C. NELSON — *Proc. USAEC Symp. on Zirconium Alloy Development*, Report GEAP-4089 (1962).
- 33 Report AECL — 2252, May 1965.
- 34 B. COX, M. J. DAVIES and A. D. DENT — *Report AERE-M621* (1960).
- 35 R. C. ASHER, D. DAVIES, A. HALL, T. B. A. KIRSTEIN, J. W. MARRIOTT and P. J. WHITE — *Electrochem. Techn.*, **4** : 231 (1966).
- 36 H. P. MAFFEI — *USAEC-Report HW-84 281*, 5.26-5.29.

- 37 D. R. McCLINTOCK — *Trans. Am. Nucl. Soc.*, **8** : No. 1, 17 (1965).
- 38 O. FLINT — *Corrosion*, **16** : 99 (1960).
- 39 H. CORIOU, L. GRALL, J. HURE, M. PELRAS and H. WILLERMOZ — *Report-DM-1114*, Aug. 1961.
- 40 B. COX — *UKAEA Report AERE-R 4348* (1963).
- 41 R. S. KEMPER and D. L. ZIMMERMANN — *USAEC-Report HW-52323* (TID-4 500) (1957).
- 42 L. M. HOWE and W. R. THOMAS — *CR-Met 827* (1959).
- 43 L. M. HOWE — *AECL-1024* (1960).
- 44 R. S. KEMPER and W. S. KELLY — *Am. Soc. Testing Materials Proc.*, **56** : 823 (1956).
- 45 L. M. HOWE — *CR-Met 922* (1960).
- 46 F. R. SHOBER — *Nucleonics*, **20** : 134 (1962).
- 47 S. H. BUSH, J. MOTEFF and J. R. WEIR — *Report ANS-100*, p. 178.
- 48 A. L. BEMENT jr. — Dissertation, Univ. Michigan 1963.
- 49 D. B. SCOTT — *USAEC-Report WCAP-3269-41*, May 1965.
- 50 J. E. IVRIN — *USAEC-Report HW-84281*, 4.14-4.15.
- 51 M. C. FRASER — *USAEC-Report HW-81984*.
- 52 N. F. PRAVDYUK *et al.* — A/conf. 15/b-2052, *Proc. 2nd. Intern. Conf. Atom. Energy, Geneva*, **5** : 457 (1958).
- 53 C. R. CUPP — *J. Nucl. Mat.*, **6** : 241 (1961).
- 54 H. KOSTRON — *Arch. Eisenhüttenwesen*, **22** : 317 (1951).
- 55 D. L. DOUGLASS — *Nuclear Metallurgy*, **VII** : 19 (1961).
- 56 W. JUNG-KÖNIG, H. RICHTER, W. SPALTHOFF and E. STARKE — EURATOM-contract No. 092-62-7 RDD; Final Report Oct. 14, 1964.
- 57 M. R. LOUTHAN jr. and R. P. MARSHALL — *J. Nucl. Materials*, **9** : 170 (1963).
- 58 J. F. R. AMBLER — *Report AECL-2538*, March 1966.
- 59 J. E. IRVIN — *Electrochemical Techn.*, **4** : 240 (1966).
- 60 D. S. WOOD, J. WINTON and B. WATKINS — *Electrochemical Techn.*, **4** : 250 (1966).
- 61 C. E. ELLS and V. FIDLERIS — *Electrochemical Techn.*, **4** : 240 (1966).
- 62 J. E. DRALEY, J. A. AYRES, W. E. BERRY, E. HILLNER, S. P. RIDEOUT — *Proc. 3rd Intern. Conf. Atomic Energy, Geneva*, **9** : 470 (1964).

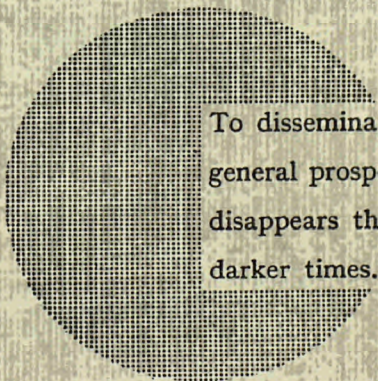
NOTICE TO THE READER

All Euratom reports are announced, as and when they are issued, in the monthly periodical **EURATOM INFORMATION**, edited by the Centre for Information and Documentation (CID). For subscription (1 year : US\$ 15, £ 5.7) or free specimen copies please write to :

Handelsblatt GmbH
"Euratom Information"
Postfach 1102
D-4 Düsseldorf (Germany)

or

Office central de vente des publications
des Communautés européennes
2, Place de Metz
Luxembourg



To disseminate knowledge is to disseminate prosperity — I mean general prosperity and not individual riches — and with prosperity disappears the greater part of the evil which is our heritage from darker times.

Alfred Nobel

SALES OFFICES

All Euratom reports are on sale at the offices listed below, at the prices given on the back of the cover (when ordering, specify clearly the EUR number and the title of the report, which are shown on the cover).

OFFICE CENTRAL DE VENTE DES PUBLICATIONS DES COMMUNAUTES EUROPEENNES

2, place de Metz, Luxembourg (Compte chèque postal N° 191-90)

BELGIQUE — BELGIË

MONITEUR BELGE
40-42, rue de Louvain - Bruxelles
BELGISCH STAATSBAD
Leuvenseweg 40-42 - Brussel

LUXEMBOURG

OFFICE CENTRAL DE VENTE
DES PUBLICATIONS DES
COMMUNAUTES EUROPEENNES
9, rue Goethe - Luxembourg

DEUTSCHLAND

BUNDESANZEIGER
Postfach - Köln 1

NEDERLAND

STAATSDRUKKERIJ
Christoffel Plantijnstraat - Den Haag

FRANCE

SERVICE DE VENTE EN FRANCE
DES PUBLICATIONS DES
COMMUNAUTES EUROPEENNES
26, rue Desaix - Paris 15°

ITALIA

LIBRERIA DELLO STATO
Piazza G. Verdi, 10 - Roma

UNITED KINGDOM

H. M. STATIONERY OFFICE
P. O. Box 569 - London S.E.1

EURATOM — C.L.D.
51-53, rue Belliard
Bruxelles (Belgique)